

Fast Imaging of Freezing Drops: No Preference for Nucleation at the Contact Line

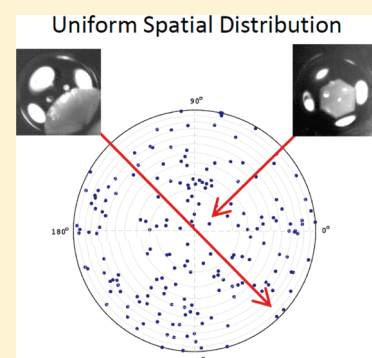
Colin Gurganus, Alexander B. Kostinski, and Raymond A. Shaw*

Atmospheric Sciences Program and Department of Physics, Michigan Technological University, Houghton, Michigan 49931, United States

S Supporting Information

ABSTRACT: We employ high-speed imaging of supercooled water drops to study the recently reported phenomenon of surface crystallization. Our geometry avoids the “point-like contact” of prior experiments by providing a simple, symmetric contact line (triple line defined by the substrate–liquid–air interface) for a drop resting on a homogeneous silicon substrate. Furthermore, the imaging configuration localizes nucleation sites in the horizontal plane so that their spatial distribution can be examined directly for possible preference near the contact line. Additionally, by using low cooling rates and avoiding substrate cooling, our design minimizes temperature variation within the water drop. The 189 freezing events display nearly perfect spatial uniformity in the immersed (liquid–substrate) region and, thereby, no preference for nucleation at the triple line. This is in contrast to prior experiments where a strong preference for surface freezing (in the contact mode) was observed.

SECTION: Atmospheric, Environmental and Green Chemistry



Supercooled metastable liquids are ubiquitous but eventually nucleate the thermodynamically stable solid phase. Whether the nucleation occurs with the help of a foreign substance (heterogeneous nucleation) or without it (homogeneous nucleation), uniform probability of cluster formation is typically assumed, scaling with surface area and volume, respectively. Recently, however, the volume scaling for homogeneous nucleation has been questioned in favor of crystallization occurring preferentially at the liquid surface (e.g., liquid–vapor interface). If so, homogeneous nucleation rates should scale with surface area rather than volume.^{1–8} Specifically for water, conflicting evidence has mounted regarding the possible preference for surface crystallization.^{1,6,9} The question is not merely academic as, for example, prediction of crystallization rates in supercooled atmospheric clouds is essential for understanding Earth’s radiation balance.¹⁰

Studies of heterogeneous nucleation also suggest a possible interfacial enhancement. It was recently observed, for example, that particles immersed in a supercooled water drop initiated freezing at temperatures 3–5 K higher in the vicinity of the air–water interface than in bulk water.^{11–13} The apparently related phenomenon of contact freezing (dry, ice-nucleating particle contacting a supercooled cloud drop) has long been observed to be more efficient than immersion nucleation.¹⁰ These observations stimulated, in part, the theoretical work of Sear,¹⁴ who used a simple Potts model to show that nucleation can favor the contact or triple lines (analogous to the substrate–water–air contact line). Preference for triple line nucleation was also observed in experiments by Suzuki et al.¹⁵ Djikaev and Ruckenstein¹⁶

conjectured that line tension could explain such a preference. In contrast, the observation of disordered layers at the ice–air interface¹⁷ might suggest that interfaces would not be preferred for ice formation. Given the importance of heterogeneous ice nucleation and the paucity of data, we have devised a different approach to study the role of the triple line in heterogeneous nucleation.

Theoretical developments have taken thermodynamic equilibrium for granted, but it should be observed that continuously cooled drops are not in thermal equilibrium. Furthermore, evidence for the enhanced interface contribution to heterogeneous nucleation comes from localized, point-like contact between the drop and seed particle, whereas the notion of surface crystallization is more fundamental and need not involve such asymmetric disturbances. Toward a cleaner test of possible contact nucleation and the line tension conjecture, we have developed an experimental approach that (i) avoids asymmetric localized contact, thereby disentangling the notion of line tension from the contact, per se, (ii) addresses the preferential nucleation mode (immersion versus contact) directly in terms of the spatial distribution of nucleation sites rather than in terms of temperature differences, (iii) has a simple symmetric and clearly defined triple line, (iv) decouples the heat sink from the nucleating region, and (v) minimizes temperature variation within the drop. The original motivation came from Sear’s¹⁴ simple geometry,

Received: April 4, 2011

Accepted: May 24, 2011

Published: May 27, 2011

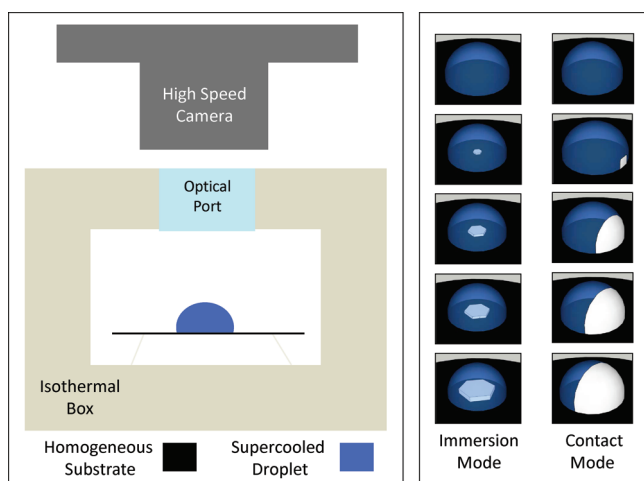


Figure 1. Experimental design and nucleation geometry. (Left) Schematic side view of the experimental setup. The high-speed camera is configured to pinpoint locations of freezing events on the substrate. The drop rests on a clean homogeneous and isothermal silicon wafer. The droplet and substrate are encased in an isothermal box, and the walls cool slowly, thereby minimizing temperature gradients. (Right) Schematic perspective view of two freezing drops, illustrating an interior substrate event (immersion mode) and an event occurring at the triple line (contact mode).

water vapor and supercooled water in contact with a uniform nucleation substrate (i.e., constant nucleation rate over the surface). Also, to ensure equal opportunity for nucleation throughout the supercooled water, it is essential to minimize temperature gradients within the drop. Indeed, we note that water density and surface tension, in addition to the nucleation rate, are temperature-dependent. Therefore, it is conceivable that heat fluxes, particularly at point contacts, may influence nucleation. This is why we formulate the contact versus immersion nucleation problem geometrically; is there a statistical preference for nucleation on the triple line in the spatial distribution of nucleation sites? This way of asking the question avoids the notion of nucleation rate and its temperature dependence altogether.

In the present experiment, rather than placing a small seed particle at the surface (i.e., at the liquid–air interface or contact mode) or inside of the droplet (i.e., immersion mode), we let the substrate act as the nucleation medium. The geometry is simple; a supercooled water droplet rests on a uniform, isothermal ice-nucleating substrate, such that initial ice formation can occur either at the liquid water–substrate interface or at the liquid water–substrate–air triple line (see Figure 1). By selecting a clean homogeneous substrate, we can remove the uncertainties associated with traditional seed particles and provide a spatially uniform probability for freezing. The freezing can be initiated anywhere within the drop–substrate interface, and a high speed movie of the freezing process localizes the nucleation site, as illustrated in Figure 1 (right panel). Over repeated cycles of freezing and melting, we determine statistically whether freezing tends to prefer the two-phase interface or the triple line.

Implicit throughout the literature is the notion that drops possess a definite temperature. We observe, however, that this is not so for heterogeneous nucleation experiments, where water drops are cooled at some finite rate $\lambda = dT/dt$. Drops cannot adjust instantly to changes in ambient temperature, but rather, temperature gradients and heat fluxes develop within the drop.

Are these negligible, or do they influence nucleation phenomena? To estimate the gradients, note that if an ambient temperature is changed suddenly, and subsequently maintained, the drop approaches a new equilibrium exponentially, with the time constant $\tau = d^2/\chi$, where χ is the thermal diffusivity, d is the drop diameter, and τ is known as the thermal relaxation time in the heat transfer literature (approximately 9 s for a $d = 1$ mm supercooled water drop). In Figure 2, we introduce the characteristic thermal variation parameter, $\Delta T \approx \lambda \tau$ and survey various experiments (including the present one) from this perspective. Because of thermal gradients, the colder portion of the volume will be favored for ice nucleation to some extent. How small should temperature variation within the drop be? On the basis of observations as well as theoretical estimates from classical nucleation theory, we adopt a tolerance of 0.1 K (see Figure 2), corresponding to approximately 10% variation in the nucleation rate for typical supercooling.¹⁸

To minimize the thermal variation in our study, (i) air itself is used to cool the drop and the substrate inside of an isothermal container, decoupling the nucleating region (the substrate) from the heat sink (see Figure 1), and (ii) a low cooling rate is used. Specifically, for our drop sizes ($V = 5 \text{ mm}^3$) with $\chi \approx 0.1 \text{ mm}^2/\text{s}$,¹⁹ we obtain a characteristic time of $\tau \approx 30$ s. Therefore, to maintain a temperature variation of $\Delta T = 0.1$ K, we must limit the cooling rate $\lambda = \Delta T/\tau$ to approximately 0.2 K/min. In this regime, the spatial temperature distribution within our sample volume can be regarded as quasi-steady, governed by Laplace's equation $\nabla^2 T = 0$ with time-dependent boundary conditions. To that end, we use isothermal walls and the maximum (Dirichlet) principle to ensure thermal homogeneity within the entire chamber.

This experiment depends primarily on our ability to determine the location of the initial nucleation site within our sample droplets. In order to achieve a suitably high frame rate (20 000 frames per second), we must subsample the CMOS sensor of our camera to 256×256 pixels, resulting in spatial resolution of $\sim 250 \mu\text{m}$ (or 5 pixels at $\sim 50 \mu\text{m}/\text{pixel}$). It is assumed that ice is formed via heterogeneous nucleation at the substrate. This assumption is reasonable as our freezing temperature limit ($T_{\text{Freeze}} > -22 \text{ }^\circ\text{C}$) is well above the homogeneous nucleation threshold of approximately $-35 \text{ }^\circ\text{C}$.²⁰ As a further test, a right angle mirror was placed near the droplet during several test runs with a $5 \mu\text{L}$ drop. We observed a delay between the nucleation event and the propagation of the freeze front to the top of the droplet. While we were unable to observe the very bottom layer of the droplet with the mirror, these observations rule out nucleation in the upper volume of the droplet.

Examples of sequential frames taken from typical freezing events are shown in Figure 3. The initial location of nucleation and the freezing “front” progression are marked by the shift in opacity during the phase transition. The left column shows frames from a movie of a freezing event that initiated, as nearly as we can determine, at the triple line (i.e., analogous to surface crystallization or contact nucleation). The right column shows the progression of a freezing event initiated in the two-phase contact region (i.e., analogous to immersion nucleation).

Over the 189 freezing events, we observed both contact and immersion nucleation events. The distribution of nucleation sites is shown in Figure 4 (top panel), and it appears to be uniform, with no obvious preference for the perimeter (the triple line). This can be quantified by sorting events into equal area zones, with the minimum width determined by our spatial resolution (approximately 5% of drop radius), as shown in the bottom panel

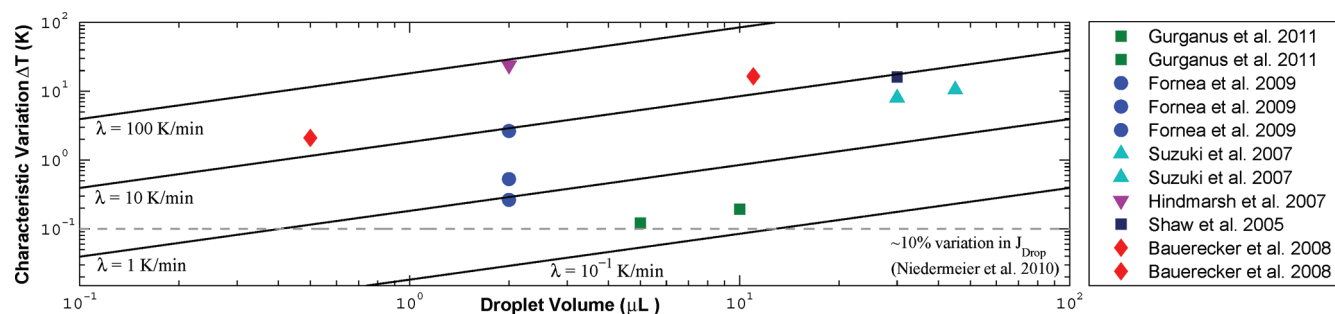


Figure 2. Deviation from thermal homogeneity (equilibrium) within drops, subjected to steady cooling. Here, we present likely thermal variations ΔT for various experiments, estimated on the basis of thermal relaxation time τ and applied cooling rate λ . The thermal relaxation time is estimated using a characteristic length scale $V^{1/3}$ (for aspherical drops). Contours of the experimental control parameter λ are also shown. Points are shown for the conditions of the homogeneous experiments of Bauerecker⁶ (1.5 and 4.5 mm acoustically levitated drops placed in a chilled volume, with a cooling rate of 20 K/min estimated from their Figure 3; droplets had varying salt concentrations) and Hindmarsh⁴ (spherical droplet suspended from a thermocouple with a cooling rate of 90 K/min, as estimated from their Figure 2; droplets had varying sucrose concentrations), as well as the heterogeneous experiments (spherical cap droplets on an actively cooled substrate) of Fornea,¹³ Gurganus (presented here), Shaw,¹¹ and Suzuki.¹⁵

of Figure 4. For a uniform distribution, we expect Poisson-distributed counts, with 19 events per zone, as shown by the solid horizontal line, and a variance (equal to the mean) as denoted by the dashed horizontal lines. The observed variability is within this range, and most importantly, the 10th bin (corresponding to likely contact nucleation events) is well within the bound.

On the basis of prior experiments,^{11–13,15} we anticipated nucleation to occur preferentially at the triple line. Thus, a surprising result of the current experiment is the observed statistical uniformity, the absence of preferential nucleation along the drop perimeter or “contact” mode. Could this result be attributed to an experimental flaw or an artifact (e.g., surface irregularities or dust on the substrate) acting as “preferred sites” for immersion nucleation? While this cannot be ruled out entirely, we observe that the nucleation site migrates around the substrate during repeated freezes of an individual droplet, which would not be expected if an energetically preferred nucleation site was present. Occasionally, we did observe consecutive, coincident-in-space freezing events, presumably due to external contamination. All such coincident events were eliminated from further analysis.

So why was surface crystallization observed in such a striking way in prior heterogeneous experiments^{11–13,15} but absent in the current study? Before confronting the notion of surface crystallization and the line tension conjecture prevalent in the recent literature, it is important to review the difference between this and earlier experiments. In some of the earlier experiments, the contact was highly localized,^{11–13} but in the current study, the substrate is smooth, clean, and homogeneous. Perhaps, then, the localized contact somehow promotes nucleation in its vicinity. Support for this view can be found in a recent study where roughness of the substrate was the crucial characteristic.⁸ Also, the heat sink and nucleating regions were decoupled in the current experiments, and thermal gradients were softened by using a very low cooling rate. Indeed, while Suzuki et al.¹⁵ used a similar geometry (droplet on homogeneous silicon substrate), they used substrate cooling. Their main observation of preferential nucleation at the triple line is contrary to ours. Perhaps it is the thermal gradients and associated heat fluxes^{21,22} that somehow provoked or triggered nucleation in earlier experiments (although, for example, Shaw et al. and Fornea et al. observed similar enhancements for rather different cooling rates).

Another possibility of reconciling the current null result with prior observations from point-like contact experiments^{11–13} is

suggested by the vast difference in the extent of the contact line. If there exists a distinct nucleation rate for freezing at the triple line, it is presumably proportional to the contact length. The extensive nucleation rate (expressed as the number of freezing events per unit time) can then be written as the sum of contributions from immersion and contact modes $J_i A + J_c P$, where J denotes intensive nucleation rate and A and P are the liquid–substrate area and air–liquid–substrate perimeter. The relative role of immersion versus triple line nucleation therefore scales with drop diameter in our geometry. Thus, decreasing the system size will tend to favor surface crystallization. Similarly, Duft and Leisner⁹ pointed out the relevance of the surface to volume ratio to the question of surface crystallization in homogeneous nucleation. Their measurements of nucleation waiting time distributions allowed for an upper bound to be placed on the surface crystallization rate, but this is not possible in our work without appeal to a nucleation theory to provide the temperature dependence.

The preceding argument is purely geometric and need not involve details of the nucleation rates. However, one can specialize further. The energetic arguments of Djikaev and Ruckenstein¹⁶ suggest a dependence of heterogeneous surface crystallization on the triple line tensions (ice–liquid–substrate, ice–air–substrate, liquid–air–substrate). An ice nucleus forming at the contact line presumably leads to a reduction in the nucleation barrier proportional to the product of the resulting change in line tension and the size of the nucleus. The possible importance of line tension for heterogeneous nucleation has also been pointed out before,²³ but line tension values remain poorly characterized (even the sign²⁴ and existence²⁵). We can gain some tentative insight through scale analysis; for a supercooled droplet (spherical cap geometry), the ratio of the line tension and surface tension contributions to free energy scales as τ/σ .²⁴ Taking $\sigma \approx 0.1 \text{ J m}^{-2}$ and $\tau \approx 10^{-10} \text{ J m}^{-1}$,^{26,27} the ratio τ/σ is on the order of 1 nm. This hints that exceedingly small system sizes may be required before line tension becomes significant. In the prior experiments,^{11–13} fine-scale imperfections on the ice-nucleating particles likely existed, and line tension may have been important. The question remains open.

EXPERIMENTAL METHODS

The experiment design (shown schematically in Figure 1, left panel) consists of a cylindrical volume with copper-lined, actively

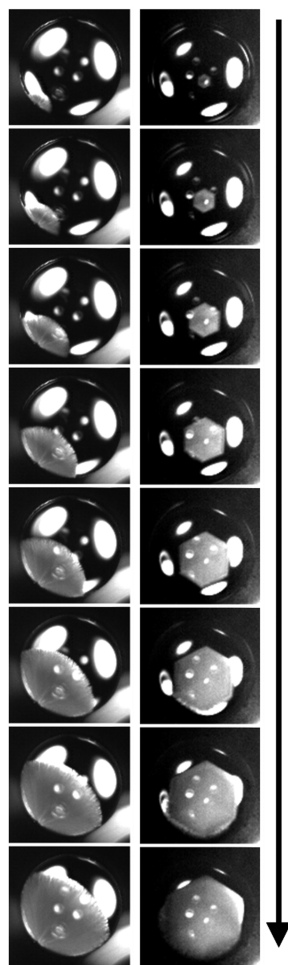


Figure 3. Progressions (time evolves downward) of contact (left) and immersion (right) nucleation events for a $10\ \mu\text{L}$ spherical cap droplet, viewed from above. The images have been enhanced for contrast, with the freezing front appearing in gray and bright LED reflections evident. In the immersion film, the nucleated crystal is oriented with the basal plane aligned with the imaging plane, thereby showing a hexagonal shape, but this is not necessarily the preferred orientation. These videos were recorded at 20 000 frames per second, with every 20th frame displayed (0.001s time steps between images). A movie of the two freezing events (played at 6×10^{-4} times live speed) is available as Supporting Information.

cooled walls and a small optical window at the top. Wall temperatures are regulated via a circulated ethylene glycol solution from a Neslab RTE-140 Chiller. A humidified nitrogen supply line can increase the relative humidity when $T > 273\ \text{K}$, but sample runs are typically limited by evaporation to 12–20 freeze–thaw cycles before the droplet must be replaced. The temperature and humidity within the volume are recorded with a RTD (via a Lakeshore 331), and a capacitive polymer sensor (Precon HS-2000D). Our experiments were performed with both p- and n-doped 2.5 cm diameter atomically smooth silicon wafers (Wafer World, Inc., test grade, 250–300 μm thick). No difference in nucleating properties between p and n substrates was observed. The silicon wafers were washed with copious amounts of distilled water and then acetone and dried with a clean nitrogen flow. After the wafer was placed in the chamber, a 5 or $10\ \mu\text{L}$ droplet of type 1 grade water (distilled, deionized, UV-irradiated) was placed on its center, and the chamber was

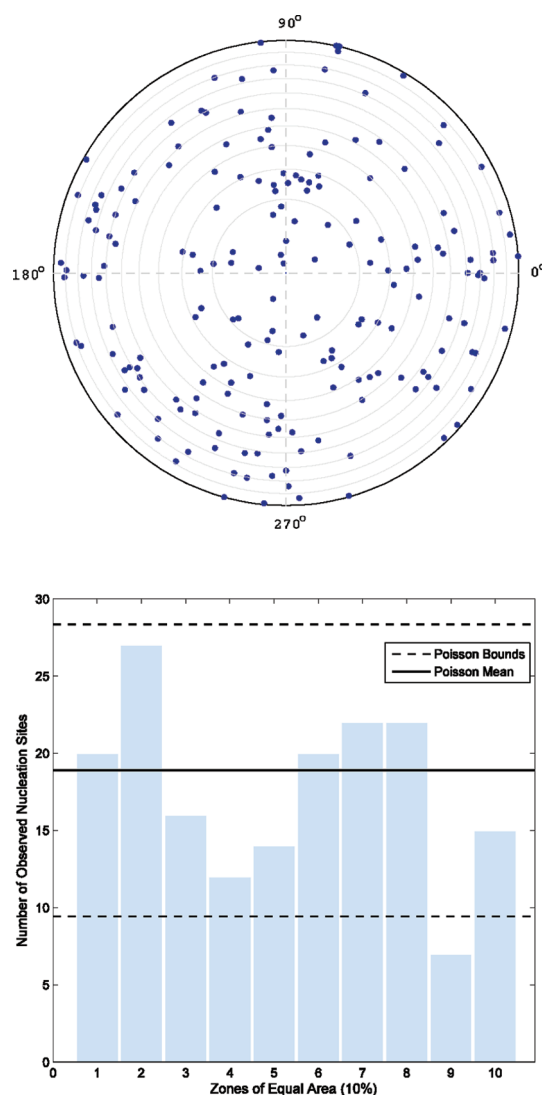


Figure 4. Evidence for spatial uniformity of nucleation events. Contrary to expectations, there is no preference for perimeter (contact mode) nucleation. (Top) Locations of the 189 freezing events on the horizontal plane. Radial positions have been scaled by drop radius to facilitate comparison between runs. (Bottom) An equal area histogram of 10 circular bands provides a quantitative measure of spatial uniformity. The solid horizontal line denotes the expected number of events per bin (19) assuming uniform distribution, and the dashed horizontal lines mark the Poisson bounds.

sealed. Lastly, a humidified nitrogen flow of $1\ \text{L}\ \text{min}^{-1}$ was used to purge the chamber, prior to initiation of the chilling cycle.

In practice, the chamber is cooled in two stages, (i) quick cooling to minimize evaporation ($\lambda = 0.3\text{--}0.5\ \text{K}\ \text{min}^{-1}$) and, once the likely freezing range is attained, (ii) a slower cooling rate ($\lambda = 0.13\text{--}0.25\ \text{K}\ \text{min}^{-1}$), without airflow into the volume. The notion of thermal relaxation time can be applied to the chamber as a whole. The thermal diffusivity of air is approximately $0.2\ \text{cm}^2\ \text{s}^{-1}$, so that for our chamber dimensions of 4 cm, the temperature difference between the wall and the interior is about 1 K. This lag of $\lambda\tau_{\text{air}} \approx 1\ \text{K}$ between the actively cooled walls and the interior is indeed confirmed by simultaneous temperature measurements.

We recorded a video of each freeze and determined the location of the initial nucleation site. A high-speed Phantom

v7.3 camera continuously recorded the droplet (through the window above the droplet; see Figure 1) when the chamber's temperature entered the freezing regime. Illumination was provided by LEDs suspended from the top section of the chamber. We have also developed an optical triggering system, which initiates a transfer of the images in the camera's ring buffer when a freezing event is detected. After the data are transferred, a heating cycle warms the chamber volume to 276 K to melt the droplet before the cooling cycle is repeated.

The observed mean freezing temperature of the drops is $-18\text{ }^{\circ}\text{C}$. The chamber contains a water reservoir that freezes earlier than the drop (at approximately $-5\text{ }^{\circ}\text{C}$); therefore, at the time of drop freezing, the relative humidity is close to 100% with respect to ice. The drops slowly evaporate during the repeated freezing and melting cycles, losing roughly half of their mass over a 36 h period. An upper bound on the resulting evaporative cooling rate, obtained by neglecting heat transfer into the drop from the air or substrate, can be estimated as $(L/c)(1/m)(dm/dt) \approx 0.1\text{ K/min}$, where L and c are the latent heat of vaporization and the specific heat of water, respectively, and m is the drop mass. This is of the same order as the chamber cooling rate, and in practice, the thermal gradients driving heat transfer are overwhelmingly confined to the surrounding air rather than the water because the thermal diffusivity of air is greater by a factor of approximately 100. Heating due to the LED illumination is estimated from the emission spectrum and the wavelength-dependent complex refractive index of water.²⁸ Unlike evaporation, the heating is uniform throughout the drop because of the very low absorption coefficient of water. Accounting for the LED efficiency, the resulting heating rate for a $10\text{ }\mu\text{L}$ droplet is approximately 0.02 K/min , roughly an order of magnitude less than the chamber cooling rate.

■ ASSOCIATED CONTENT

S Supporting Information. The full movie for the nucleation events in Figure 3. This material is available free of charge via the Internet at <http://pubs.acs.org>.

■ AUTHOR INFORMATION

Corresponding Author

*E-mail: rashaw@mtu.edu.

■ ACKNOWLEDGMENT

The authors would like to thank E. Bodenschatz and Z. Warhaft (Cornell University) for use of the Phantom v7 camera. Helpful discussions with W. Cantrell and R. Sear are appreciated. A.B.K. wishes to thank the staff of Environmental Sciences Department, Weizmann Institute of Science, for hospitality and support. This research was supported in part by an award from the Department of Energy (DOE) Office of Science Graduate Fellowship Program administered by the Oak Ridge Institute for Science and Education for the DOE. ORISE is managed by Oak Ridge Associated Universities (ORAU) under DOE Contract Number DE-AC05-06OR23100. All opinions expressed in this paper are the authors' and do not necessarily reflect the policies and views of DOE, ORAU, or ORISE. This work was also supported in part by the National Science Foundation, Grants ATM05-54670 and AGS-1026123.

■ REFERENCES

- (1) Tabazadeh, A.; Dijkstra, Y. S.; Reiss, H. Surface Crystallization of Supercooled Water in Clouds. *Proc. Natl. Acad. Sci. U.S.A.* **2002**, *99*, 15873–15878.
- (2) Dijkstra, Y. S.; Tabazadeh, A.; Hamill, P.; Reiss, H. Thermodynamic Conditions for the Surface-Stimulated Crystallization of Atmospheric Droplets. *J. Phys. Chem. A* **2002**, *106*, 10247–10253.
- (3) Ciobanu, V. G.; Marcolli, C.; Krieger, U. K.; Zuend, A.; Peter, T. Efflorescence of Ammonium Sulfate and Coated Ammonium Sulfate Particles: Evidence for Surface Nucleation. *J. Phys. Chem. A* **2010**, *114*, 9486–9495.
- (4) Hindmarsh, J. P.; Russell, A. B.; Chen, X. D. Observation of the Surface and Volume Nucleation Phenomena in Undercooled Sucrose Solution Droplets. *J. Phys. Chem. C* **2007**, *111*, 5977–5981.
- (5) Sutter, P. W.; Sutter, E. A. Dispensing and Surface-Induced Crystallization of Zeptolitre Liquid Metal–Alloy Drops. *Nature Mat.* **2007**, *6*, 363–366.
- (6) Bauerecker, S.; Ulbig, P.; Buch, V.; Vrbka, L.; Jungwirth, P. Monitoring Ice Nucleation in Pure and Salty Water via High-Speed Imaging and Computer Simulations. *J. Phys. Chem. C* **2008**, *112*, 7631–7636.
- (7) Li, T.; Donadio, D.; Ghiringhelli, L. M.; Galli, G. Surface-Induced Crystallization in Supercooled Tetrahedral Liquids. *Nat. Mater.* **2009**, *8*, 726–730.
- (8) Carvalho, J. L.; Dalnoki-Veress, K. Homogeneous Bulk, Surface, and Edge Nucleation in Crystalline Nanodroplets. *Phys. Rev. Lett.* **2010**, *105*, 237801.
- (9) Duft, D.; Leisner, T. Laboratory Evidence for Volume-Dominated Nucleation of Ice in Supercooled Water Microdroplets. *Atmos. Chem. Phys.* **2004**, *4*, 1997–2000.
- (10) Cantrell, W.; Heymsfield, A. Production of Ice in Tropospheric Clouds: A Review. *Bull. Am. Meteorol. Soc.* **2005**, *86*, 795–807.
- (11) Shaw, R. A.; Durant, A. J.; Mi, Y. Heterogeneous Surface Crystallization Observed in Undercooled Water. *J. Phys. Chem. B* **2005**, *109*, 9865–9868.
- (12) Durant, A. J.; Shaw, R. A. Evaporation Freezing by Contact Nucleation Inside-Out. *Geophys. Res. Lett.* **2005**, *32*, L20814.
- (13) Fornea, A. P.; Brooks, S. D.; Dooley, J. B.; Saha, A. Heterogeneous Freezing of Ice on Atmospheric Aerosols Containing Ash, Soot, and Soil. *J. Geophys. Res.* **2009**, *114*, D13201.
- (14) Sear, R. P. Nucleation at Contact Lines Where Fluid–Fluid Interfaces Meet Solid Surfaces. *J. Phys.: Condens. Matter* **2007**, *19*, 466106.
- (15) Suzuki, S.; Nakajima, A.; Yoshida, N.; Sakai, M.; Hashimoto, A.; Kameshima, Y.; Okada, K. Freezing of Water Droplets on Silicon Surfaces Coated with Various Silanes. *Chem. Phys. Lett.* **2007**, *445*, 37–41.
- (16) Dijkstra, Y. S.; Ruckenstein, E. Thermodynamics of Heterogeneous Crystal Nucleation in Contact and Immersion Modes. *J. Phys. Chem. A* **2008**, *112*, 11677–11687.
- (17) Goertz, M. P.; Zhu, X.-Y.; Houston, J. E. Exploring the Liquid-Like Layer on the Ice Surface. *Langmuir* **2009**, *25*, 6905–6908.
- (18) Niedermeier, D.; Hartmann, S.; Shaw, R. A.; Covert, D.; Mentel, T. F.; Schneider, J.; Poulain, L.; Reitz, P.; Spindler, C.; Clauss, T.; et al. Heterogeneous Freezing of Droplets with Immersed Mineral Dust Particles — Measurements and Parameterization. *Atmos. Chem. Phys.* **2010**, *10*, 3601–3614.
- (19) Benchikh, O.; Fournier, D.; Boccaro, A. C. Photothermal Measurement of the Thermal Conductivity of Supercooled Water. *J. Phys. (Paris)* **1985**, *46*, 727–731.
- (20) Pruppacher, H. R.; Klett, J. D. *Microphysics of Clouds and Precipitation*; Kluwer Academic Publishers: Boston, MA, 1997; p 213.
- (21) Kostinski, A.; Cantrell, W. Entropic Aspects of Supercooled Droplet Freezing. *J. Atmos. Sci.* **2008**, *65*, 2961–2971.
- (22) de Gennes, P.-G.; Brochard-Wyart, F.; Quere, D. *Capillarity and Wetting Phenomena*; Springer: New York, 2004; sec. 10.2.1.
- (23) Evans, L. F.; Lane, J. E. Line Tension and Ice Nucleation Theory. *J. Atmos. Sci.* **1973**, *30*, 326–331.

(24) Berg, J. K.; Weber, C. M.; Riegler, H. Impact of Negative Line Tension on the Shape of Nanometer-Size Sessile Droplets. *Phys. Rev. Lett.* **2010**, *105*, 076103.

(25) de Gennes, P.-G.; Brochard-Wyart, F. Quere, D. *Capillarity and Wetting Phenomena*; Springer: New York, 2004; sec. 3.2.1.

(26) Rowlinson, J. S.; Widom, B. *Molecular Theory of Capillarity*; Clarendon Press: Oxford, U.K., 1982; sec. 8.6.

(27) Marmur, A. Line Tension and the Intrinsic Contact Angle in Solid–Liquid–Fluid Systems. *J. Colloid Interface Sci.* **1997**, *186*, 462–466.

(28) Bohren, C. F.; Huffman, D. R. *Absorption and Scattering of Light by Small Particles*; John Wiley & Sons: New York, 1983; sec. 10.3.